*IN-20*

*110094*

*P- 13*

# O$_2$ Reduction at the IFC Modified O$_2$ Fuel Cell Electrode

William L. Fielder, Joseph Singer,
and Richard S. Baldwin
*Lewis Research Center*
*Cleveland, Ohio*

and

Richard E. Johnson
*LeTourneau University*
*Longview, Texas*

**NASA**

N92-29667

Unclas
G3/20   0110094

# $O_2$ REDUCTION AT THE IFC MODIFIED $O_2$ FUEL CELL ELECTRODE

William L. Fielder, Joseph Singer, and
Richard S. Baldwin
National Aeronautics and Space Administration
Lewis Research Center
Cleveland, Ohio 44135

Richard E. Johnson
LeTourneau University
Longview, Texas 75601

## SUMMARY

The International Fuel Cell Corporation (IFC) state-of-the-art (SOA) $O_2$ electrode (Au-10%Pt electrocatalyst by weight) is currently being used in the alkaline $H_2$–$O_2$ fuel cell in the NASA Space Shuttle. Recently, IFC has developed an improved $O_2$ electrode, designated as the IFC modified $O_2$ electrode, as a possible replacement for the SOA electrode.

In the present study, $O_2$ reduction data were obtained for the modified electrode at temperatures between 23.3 and 91.7 °C. BET measurements gave an electrode BET surface area of about 2070 $cm^2/cm^2$ of geometric surface area. The Tafel data could be fitted to two straight line regions. The slope for the lower region, designated as the 0.04 V/decade region, was temperature dependent, and the transfer coefficient was about 1.5. The "apparent" energy of activation for this region was about 19 kcal/mol. An $O_2$ reduction mechanism for this 0.04 region is presented. In the upper region, designated as the 0.08 V/ decade region, diffusion may be the controlling process. Tafel data are presented to illustrate the increase in performance with increasing temperature.

## INTRODUCTION

Efficient electrical power systems are major requirements for space applications. For example, the International Fuel Cells Corporation (IFC) alkaline $H_2$–$O_2$ fuel cell is used as a primary energy source aboard the NASA Space Transportation System (Space Shuttle). Although the energy density of the $H_2$–$O_2$ fuel cell system is attractive, its voltage efficiency is less than 100 percent, primarily because of the slower kinetics of the $O_2$ electrode.

Initially, IFC used Pt as the electrocatalyst for the $O_2$ electrode, but the fuel cell performance decayed with time because of the gradual dissolution of Pt. Subsequently, IFC developed a more stable $O_2$ electrode by using high-surface-area Au-10%Pt (wt%) alloy powder as the electrocatalyst. This state-of-the-art (SOA) electrode is currently being used in the fuel cell on the NASA Space Shuttle. Performance and stability data have been reported for this electrode (refs. 1 and 2); Tafel slopes were 0.045 to 0.051 V/decade in 35-percent KOH (1 atm $O_2$) at 70 °C. Endurance tests at 0.215 $A/cm^2$ and 60 °C for a six-cell stack indicated that the $O_2$ electrodes were stable, with a potential decay of less than 2 $\mu$V/hr during a cyclic test of over 18 000 hr (ref. 3). Another study, in which a floating electrode half-cell apparatus was used, reported Tafel slopes of about 0.04 and 0.12 V/decade at moderate current densities for the SOA electrode (ref. 4).

Recently, IFC has developed an improved $O_2$ electrode, designated the modified $O_2$ electrode, that uses similar fine-particle Au-10%Pt as the electrocatalyst. Since IFC's preliminary results indicate improved performance, the modified electrode is being considered as a possible replacement for the SOA electrode in the NASA Space Shuttle fuel cell. This fuel cell operates at temperatures of about 60 °C;

however, for increased efficiency, it may be desirable to operate these fuel cells at temperatures above 60 °C.

The present work involved a preliminary study of the IFC modified electrode in a floating electrode half-cell apparatus over a temperature range of about 65 °C. The $O_2$ reduction performance data obtained between 23.3 and 91.7 °C showed that electrode performance increased with temperature. A mechanism for the $O_2$ reduction is presented herein.

## EXPERIMENT

### Electrode Fabrication

A sample of the IFC modified $O_2$ electrode was obtained from IFC. Although IFC considers the details of the electrode's fabrication and structure to be proprietary, some information was available. The surface area of the Au-10%Pt alloy powder was about 15 m$^2$/g. IFC had mixed the powder with a polytetrafluoroethylene (PTFE) suspension and pressed the mixture onto a grated thin foil Au current collector equivalent to a 100-mesh screen. The resulting "green" electrode was dried and sintered into a network to produce a PTFE-bonded electrode. IFC optimized this electrode with the desired hydrophilic-hydrophobic character to maximize $O_2$ gas diffusion to the catalyst-electrolyte interface while minimizing electrode flooding.

### Surface Area and Capacitance

A Beta Scientific Automatic Surface Analyzer (Model 4200) was used to measure the BET surface area at 2070 cm$^2$/cm$^2$ of geometric area.

A sample of the electrode was submerged in the KOH electrolyte at 24 °C under an inert atmosphere of $N_2$. Capacitances of the Au-10%Pt powder in the modified electrode were estimated from cyclic sweeps (in the absence of $O_2$) at potentials where currents resulting from kinetic processes were small. A cyclic voltammogram was obtained at 5 mV/sec between -0.01 and 1.38 V (see fig. 1).[1] Kinetic processes appear to be minimal at about 0.1 V. Therefore, the electrode was scanned between 0.05 and 0.15 V at 1 mV/sec; this voltammogram is shown in figure 2. The capacitance can be calculated as follows:

$$C = 0.5(i_A + i_C)/S \tag{1}$$

where $i_A$ and $i_C$ represent the anodic and cathodic currents, respectively, expressed in mA; and S represents the scan rate in mV/sec. For example, anodic and cathodic currents of 0.079 and -0.333 mA were obtained at the intermediate potential of 0.10 V, giving a capcitance of about 0.13 farads/cm$^2$ of geometric area. If the double layer capacitance is assumed to be 100 $\mu$farads/cm$^2$ of electrochemical surface, about 60 percent of the BET area is being utilized.

---

[1]All potentials in the present study will refer to the reversible $H_2$ potential (RHE) unless otherwise stated.

## Experimental Apparatus

A floating electrode half-cell apparatus (see fig. 3) was used for the electrochemical studies (ref. 5). A coil of Au wire served as the counter electrode. An atmosphere of gaseous $O_2$ (or $N_2$) was passed into the half-cell apparatus through a presaturator cell that contained KOH at the same temperature and concentration as the half-cell. This minimized changes in KOH concentration due to loss of $H_2O$.

Galvanostatic current-potential measurements have been obtained manually and by means of a computer-driven system. Both methods gave virtually the same results. For the computer-driven system, the potentiostat (EG&G Princeton Applied Research Model 173) was interfaced with an Apple IIe computer by means of an EG&G Model 276 plug-in unit. A computer program (EG&G Electrochemistry Program, Vol. I) was used to drive and control the potentiostat. For the manual runs, an EG&G Model 376 plug-in unit was used with the potentiostat.

The iR polarizations were determined by means of an Electrosynthesis Corporation IR instrument (Model 800) in conjunction with a 7-V Zener diode. This instrument periodically interrupted the current for an interval of a few microseconds, and the diode limited the voltage rise to 7 V during the interruption.

## Experimental Procedure

A Hg/HgO electrode served as the reference electrode. Its potential at 25 °C was 0.926 V. The temperature coefficient for this Hg/HgO electrode (see fig. 4) was about -0.45 mV/ °C, as determined by comparing its potentials at various temperatures with those of a dynamic $H_2$ electrode.

A sample of the modified electrode (1.60 $cm^2$ of geometric area) was introduced into the half-cell apparatus as the working electrode, with its catalyst side contacting the 30-percent KOH electrolyte surface. The electrode was raised slightly to form a small meniscus at the electrode-electrolyte interface. Exact positioning of the electrode is not critical for determining iR-corrected potentials. Although the potential and iR value may vary slightly with electrode positioning, the corresponding iR-corrected potential for a galvanostatic run remains virtually constant for a small meniscus height.

PTFE-bonded electrodes often require cathodic preconditioning to minimize polarization. Initially, the electrode was held cathodically at about -0.9 A for about 1 hr. Then, prior to each series of runs, the electrode was held at about -0.9 A for periods of about 0.25 to 1.5 hr.

Most galvanostatic runs were made without stirring, since no appreciable changes in potential were observed with different stirring rates at the currents used. At currents above 1 mA, steady-state conditions were usually obtained after only a few seconds. Once a steady-state condition was obtained, the potential remained virtually constant with time.

The iR corrections were obtained by plotting iR potentials as a function of current. See figure 5 for a typical run.

## RESULTS AND DISCUSSION

### $O_2$ Electrode Performance

$O_2$ reduction data were obtained between 23.3 and 91.7 °C for the IFC modified $O_2$ electrode. Polarization potentials for each run were determined by subtracting the steady-state potentials (iR-corrected) from the corresponding reversible $O_2$ electrode potentials (e.g., 1.229 V at 25 °C). Tafel plots were obtained by plotting polarization potentials as a function of the logarithms of the respective geometric current densities.

The data for each temperature run could be fitted to two straight line regions. This is illustrated by the solid lines in figures 6 and 7, which are for electrode A at 24.0 °C and electrode B at 77.8 °C, respectively. As shown in figure 6, at 24.0 °C the lower region (0.0002 to 0.16 A/cm$^2$) could be fitted with a slope of 0.0395 V/decade. This lower region is designated as the 0.04 V/decade region.

For comparison, the data reported in reference 4 for the IFC SOA $O_2$ electrode (obtained by using the floating electrode half-cell apparatus) is represented in figure 6 by a dashed line. The data for both electrodes were in reasonable agreement in this 0.04 region at current densities below about 0.07 A/cm$^2$. However, the improved electrode structure of the modified electrode is indicated by the extension of the 0.04 region to larger current densities. Note that although the upper region for the IFC SOA electrode begins at about 0.07 A/cm$^2$, the corresponding upper region for the modified electrode begins at about 0.16 A/cm$^2$.

The resulting slopes and intercepts (i.e., polarization potentials at 1 A/cm$^2$) in the 0.04 region for the modified electrode are listed in table I. The values of the slopes in this region increase with increasing temperature. This is illustrated in figure 8 where the values of the slopes are plotted as a function of temperature. The data for the modified electrode are represented in figure 8 by circles, and the best fit by the solid line. The temperature dependence for the 0.04 region was in agreement with the Tafel expression:

$$b = 2.3RT/aF \tag{2}$$

where $b$ represents the slope in V/decade, $a$ represents the transfer coefficient, and $F$ represents the faraday. A value of about 1.48 was calculated for the transfer coefficient.

For the modified electrode, not only the value of the slope increased with temperature, but also the limit for the upper current density in the 0.04 region increased with temperature. For example, the upper limit at 24.0 °C was about 0.16 A/cm$^2$, but the corresponding limit at 91.7 °C was about 0.3 A/cm$^2$. For comparison, the values of the slopes reported in reference 4 for the IFC SOA $O_2$ electrode are shown as squares in figure 8. These values are in reasonable agreement with the values obtained for the IFC modified $O_2$ electrode.

The geometric exchange current densities for the 0.04 region were calculated for the modified electrode by extrapolating to zero polarization. The results are listed in table II. These values increase with temperature, suggesting that the $O_2$ reduction process at the Au-10%Pt surface is thermally activated. In figure 9, the logarithms of the geometric exchange current densities are plotted as a function of the reciprocals of the absolute temperature. The data for the modified electrode are represented by circles, and the best fit by the solid line. The "apparent" energy of activation for such a reaction may be estimated by means of the following expression:

4

$$E_a = -2.3R[d\log i_o/d\log (1/T)] \tag{3}$$

where $E_a$ is the "apparent" energy of activation in cal/mol and $i_o$ is the geometric exchange current density (ref. 6). A slope of about -4118 $K^{-1}$ is obtained with a value of about 19 kcal/mol for the "apparent" energy of activation.
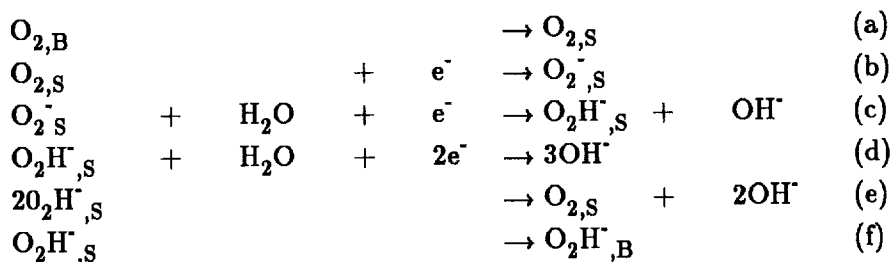
Values for the SOA electrode are represented in figure 9 by the squares; they show reasonable agreement with the best fit for the modified electrode. Since the Tafel slope values for both the SOA and the modified electrodes are similar in the 0.4 region (fig. 8), we believe that in this region similar kinetic processes are controlling the reduction of $O_2$ at the electrocatalyst surfaces of both electrodes.

A shorter straight line region with a larger slope was obtained for the modified $O_2$ electrode at higher currents (figs. 6 and 7). This region, designated in the present study as the 0.08 V/decade region, is illustrated in figure 6; here, at 24.0 °C the data between 0.18 and 0.40 $A/cm^2$ can be fitted with a straight line with a slope of about 0.084 V/decade. The data in figure 6 show that in the 0.04 region the modified electrode extends to larger current densities because of its improved electrode structure. The modified electrode, therefore, may be used at larger current densities than the SOA electrode before polarization losses become excessive.

For increased efficiency, it may be desirable to operate the IFC $H_2$–$O_2$ fuel cell at temperatures greater than 60 °C. As suggested by the polarization data, electrode performance increases with increasing temperature. This is illustrated in figure 10 where potentials (iR-corrected) for modified electrode A are plotted as a function of current at 66.1 and 90.3 °C. Furthermore, increasing the temperature to greater than 60 °C for a $H_2$–$O_2$ fuel cell system should be beneficial for minimizing iR polarization since the conductivity of 30-percent KOH increases with temperature.

## $O_2$ Reduction Mechanisms

A combination of mechanisms proposed in the literature is presented herein for $O_2$ reduction at the Au-10%Pt surface of the IFC modified electrode. In the following reactions, subscripts B and S represent, respectively, species that are in bulk and that are weakly adsorbed at the surface:

$$O_{2,B} \rightarrow O_{2,S} \tag{a}$$
$$O_{2,S} + e^- \rightarrow O_2^-{}_{,S} \tag{b}$$
$$O_2^-{}_S + H_2O + e^- \rightarrow O_2H^-{}_{,S} + OH^- \tag{c}$$
$$O_2H^-{}_{,S} + H_2O + 2e^- \rightarrow 3OH^- \tag{d}$$
$$2O_2H^-{}_{,S} \rightarrow O_{2,S} + 2OH^- \tag{e}$$
$$O_2H^-{}_{,S} \rightarrow O_2H^-{}_{,B} \tag{f}$$

The initial step for $O_2$ reduction at higher currents was reported to involve the formation of an $O_2^-$ species, as represented in reactions (a) and (b), with a Tafel slope of about 0.12 V/decade (ref. 7). A Tafel slope of about 0.04 V/decade was reported in a second study (ref. 8), which suggested that the rate-controlling step for this region involves the production of $O_2H^-$ from an intermediate in a manner similar to reaction (c).

Electrochemical reduction of $O_2H^-$ to produce $OH^-$ probably is influenced strongly by the crystal orientation of the Au surface. For example, $O_2H^-$ is reported to be electrochemically reduced at Au(100)

5

to produce OH$^-$ with a four-electron process (ref. 9); however, $O_2H^-$ is not electrochemically reduced at moderate potentials at the (110) or (111) orientations (ref. 10). A more detailed reaction scheme for determining the kinetic parameters for $O_2$ reduction at single-crystal Au, primarily involving reactions (d) to (f), was also reported (ref. 11). Even though $O_2$ is not significantly electrochemically reduced at the (110) and (111) orientations, recycling of $O_2$ at these orientations may result in an apparent electron transfer of greater than two. Some of the $O_2H^-$ produced in reaction (c) may subsequently decompose catalytically (reaction (e)) to produce OH$^-$ and $O_2$. Recycling of this $O_2$ (in reaction (b)) produces additional $O_2H^-$.

A definitive determination of the Au orientation in the IFC modified electrode cannot be made at present. However, we assume that the amount of Au(100) in this electrode is small or insignificant since Au(111) is the more stable orientation, as indicated by the formation of Au(111) after vapor deposition (ref. 12). The Au(110) and (111) orientations, therefore, may lead to an overall electron path ranging between two and four, depending on the extent of $O_2H^-$ decomposition prior to its diffusion into the bulk.

In this study of the modified electrode, reaction (c) is suggested as the rate-controlling step for the 0.04 V/decade region. The values obtained for the slopes in this region are in agreement with a predicted value of about 0.0394 V/decade for a Tafel process at 25 °C involving two consecutive one-electron transfer steps with a transfer coefficient of about 1.5 (ref. 13).

A doubling of the 0.04 value for the slope to about 0.08 V/decade was observed for the modified electrode at larger currents. It has been reported that a doubling of the slope for $O_2$ reduction at PTFE-bonded diffusion electrodes may involve a change from activation control to diffusion control (ref. 14). Thus, we believe that the 0.08 region observed for the IFC modified electrode represents a diffusion-controlled process.

## CONCLUDING REMARKS

The IFC $O_2$ electrode used in the NASA Space Shuttle alkaline $H_2$–$O_2$ fuel cell is the SOA electrode to which $O_2$ electrodes can be compared for electrocatalytic $O_2$ reduction activity. An improved electrode, designated the modified $O_2$ electrode, has been developed by IFC as a possible replacement for the SOA electrode. In the present study, preliminary data were obtained for the IFC modified electrode by using a floating electrode half-cell apparatus. A comparison of these data with similar type data reported for the IFC SOA electrode (ref. 4) indicated that the kinetic processes were similar at smaller currents, with a Tafel slope of about 0.04 V/decade for both electrodes. The improved electrode structure of the modified electrode, however, extended the 0.04 kinetic region to larger current densities before the 0.08 region became rate controlling. Polarization data indicated that electrode performance increased with increasing temperature.

## ACKNOWLEDGMENT

# REFERENCES

1. M.S. Freed and R.J. Lawrence, "Development of Gold Alloy Catalyst Cathode for Alkaline Electrolyte Fuel Cells." Paper presented at the 147th Meeting Electrochemical Society, Toronto, Canada, May 15, 1975.

2. R.E. Martin and M.A. Manzo, "Alkaline Fuel Cell Performance Investigation." NASA TM-100937, 1988.

3. R.E. Martin, J. Garow, and K.B. Michaels, "Regenerative Fuel Cell Energy Storage System for a Low Earth Orbit Space Station. Topical Report." NASA-CR-174802, 1984.

4. W.L. Fielder and J. Singer, "$O_2$ Reduction at the IFC Orbiter Fuel Cell $O_2$ Electrode." NASA TM-102580, 1990.

5. J. Giner and S. Smith, "A Simple Method for Measuring Polarization of Hydrophobic Gas Diffusion Electrodes." Electrochemical Technology, Vol. 5, No. 1-2, Jan-Feb. 1967, pp. 59-61.

6. E. Gileadi, E. Kirowa-Eisner, and J. Penciner, "Interfacial Electrochemistry. An Experimental Approach." Reading, MA: Addison Wesley, 1975 p. 74.

7. R.W. Zurilla, R.K. Sen, and E. Yeager, "The Kinetics of the Oxygen Reduction Reaction on Gold in Alkaline Solution." Journal of the Electrochemical Society, Vol. 125, No. 7, July 1978, pp. 1103-1109.

8. A. Damjanovic, M.A. Genshaw, and J.O'M. Bockris, "Hydrogen Peroxide Formation in Oxygen Reduction at Gold Electrodes. II. Alkaline Solution." Journal of Electroanalytical Chemistry and Interfacial Electrochemistry, Vol. 15, 1967, pp. 173-180.

9. R.R. Adzic, N.M. Markovic, and V.B. Vesovic, "Structural Effects in Electrocatalysis. Oxygen Reduction on the Au(100) Single Crystal Electrode." Journal of Electroanalytical Chemistry and Interfacial Electrochemistry, Vol. 165, 1984, pp. 105-120.

10. N.M. Markovic, R.R. Adzic, and V.B. Vesovic, "Structural Effects in Electrocatalysis. Oxygen Reduction on the Gold Single Crystal Electrodes with (110) and (111) Orientations." Journal of Electroanalytical Chemistry and Interfacial Electrochemistry, Vol. 165, 1984, pp. 121-133.

11. R.R. Adzic, S. Strbac, and N. Anastasijevic, "Electrocatalysis of Oxygen on Single Crystal Gold Electrodes." Materials Chemistry and Physics, Vol. 22, No. 3-4, 1989, pp. 349-375.

12. C. Paliteiro, A. Hamnett, and J.B. Goodenough, "The Electroreduction of Dioxygen on Thin Films of Gold in Alkaline Solution." Journal of Electroanalytical Chemistry and Interfacial Electrochemistry, Vol. 234, 1987, pp. 193-211.

13. A. Damjanovic, M.A. Genshaw, and J.O'M. Bockris, "The Mechanism of Oxygen Reduction at Platinum in Alkaline Solutions with Special Reference to $H_2O_2$." Journal of the Electrochemical Society, Vol. 114, No. 11, Nov. 1967, pp. 1107-1112.

14. J. Giner and C. Hunter, "The Mechanism of Operation of the Teflon-Bonded Gas Diffusion Electrode: A Mathematical Model." Journal of the Electrochemical Society, Vol. 116, No. 8, Aug. 1969, pp. 1124-1130.

TABLE I.—SLOPES AND INTERCEPTS IN THE

0.04 V/DECADE REGION FOR THE

IFC MODIFIED $O_2$ ELECTRODE

| Sample | Temperature, °C | Slope, V/Decade | Intercept, V |
|--------|--------|--------|--------|
| C | 23.3 | 0.0397 | 0.3652 |
| C | 23.9 | .0379 | .3498 |
| A | 24.0 | .0396 | .3622 |
| B | 24.0 | .0393 | .3630 |
| B | 24.0 | .0395 | .3608 |
| B | 26.6 | .0400 | .3727 |
| B | 26.9 | .0395 | .3529 |
| A | 28.1 | .0394 | .3457 |
| A | 30.8 | .0390 | .3433 |
| A | 33.3 | .0388 | .3402 |
| B | 34.7 | .0395 | .3487 |
| C | 35.3 | .0411 | .3462 |
| A | 44.4 | .0446 | .3653 |
| B | 46.1 | .0436 | .3428 |
| C | 46.9 | .0433 | .3419 |
| B | 54.4 | .0440 | .3342 |
| A | 55.0 | .0472 | .3610 |
| C | 55.3 | .0449 | .3427 |
| B | 65.6 | .0435 | .3272 |
| A | 66.1 | .0475 | .3503 |
| C | 66.4 | .0453 | .3334 |
| A | 77.2 | .0488 | .3422 |
| B | 77.8 | .0471 | .3260 |
| C | 78.3 | .0466 | .3331 |
| A | 90.3 | .0486 | .3106 |
| B | 91.7 | .0498 | .3516 |

## TABLE II.—EXCHANGE CURRENT DENSITIES IN THE 0.04 V/DECADE REGION FOR THE IFC MODIFIED $O_2$ ELECTRODE

| Temperature, °C | Reciprocal temperature, $(K)^{-1}$ | log Geometric exchange current density, $A/cm^2$ | Geometric exchange current density, $A/cm^2$ |
|---|---|---|---|
| 23.3 | 0.003375 | -9.199 | $6.32 \times 10^{-10}$ |
| 23.9 | .003368 | -9.230 | 5.89 |
| 24.0 | .003367 | -9.146 | 7.14 |
| 24.0 | .003367 | -9.237 | 5.80 |
| 24.0 | .003367 | -9.134 | 7.34 |
| 26.6 | .003338 | -9.318 | 4.81 |
| 26.9 | .003334 | -8.936 | $1.16 \times 10^{-9}$ |
| 28.1 | .003321 | -8.775 | 1.68 |
| 30.8 | .003292 | -8.801 | 1.58 |
| 33.3 | .003265 | -8.767 | 1.71 |
| 34.7 | .003250 | -8.827 | 1.49 |
| 35.3 | .003244 | -8.424 | 3.77 |
| 44.4 | .003151 | -8.190 | 6.45 |
| 46.1 | .003134 | -7.863 | $1.37 \times 10^{-8}$ |
| 46.9 | .003126 | -7.896 | 1.27 |
| 54.4 | .003054 | -7.596 | 2.54 |
| 55.0 | .003049 | -7.648 | 2.25 |
| 55.3 | .003046 | -7.633 | 2.33 |
| 65.6 | .002953 | -7.521 | 3.01 |
| 66.1 | .002949 | -7.375 | 4.22 |
| 66.4 | .002946 | -7.492 | 3.22 |
| 77.2 | .002856 | -7.012 | 9.72 |
| 77.8 | .002851 | -6.921 | $1.20 \times 10^{-7}$ |
| 78.3 | .002847 | -7.148 | $7.11 \times 10^{-8}$ |
| 90.3 | .002753 | -6.391 | $4.06 \times 10^{-7}$ |
| 91.7 | .002742 | -7.060 | $8.70 \times 10^{-8}$ |

Figure 1.—Cyclic voltammogram of modified electrode between –0.01 and 1.38 V (5mV/sec, 24 °C, 1 atm $N_2$, 1 presweep).
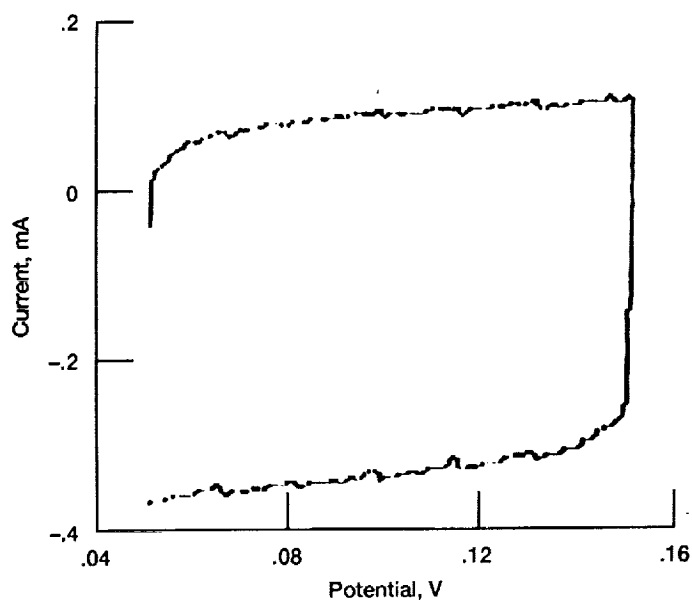


Figure 2.—Cyclic voltammogram of modified electrode between 0.05 and 0.15 V (1 mV/sec, 24 °C, 1 atm $N_2$, 1 presweep).
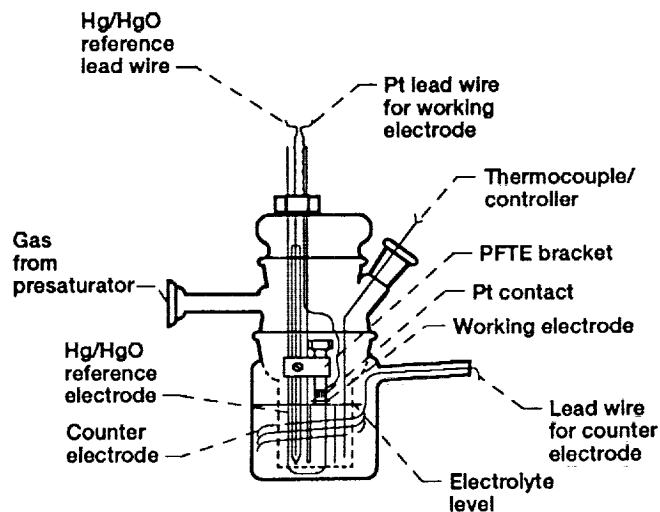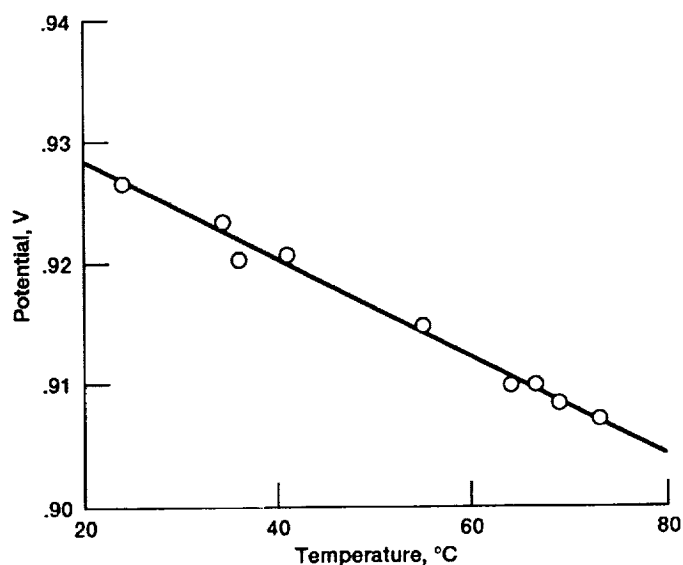


Figure 3.—Schematic of floating electrode half-cell.



Figure 4.—Hg/HgO potential with respect to temperature (1 atm $O_2$, 30 percent KOH, coefficient = – 0.45 mV/°C).
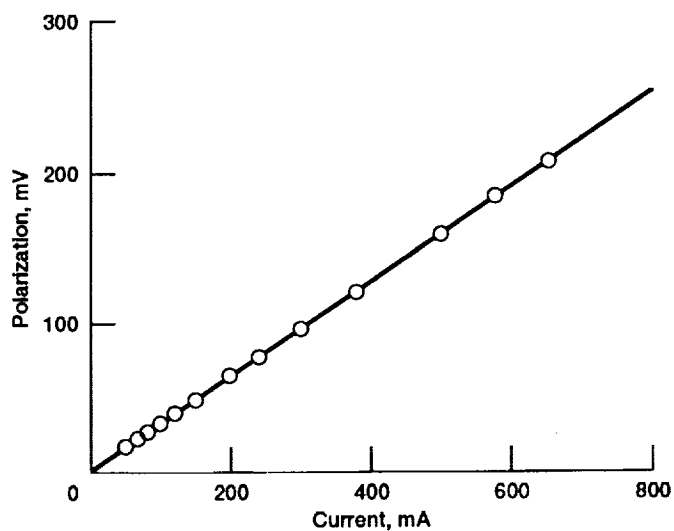


Figure 5.—The iR polarization with respect to current for $O_2$ reduction (24 °C, 1 atm $O_2$, 30 percent KOH).

10

Figure 6.—Tafel plot for $O_2$ reduction for the modified A and SOA electrodes (24 °C, 1 atm $O_2$, 30 percent KOH).
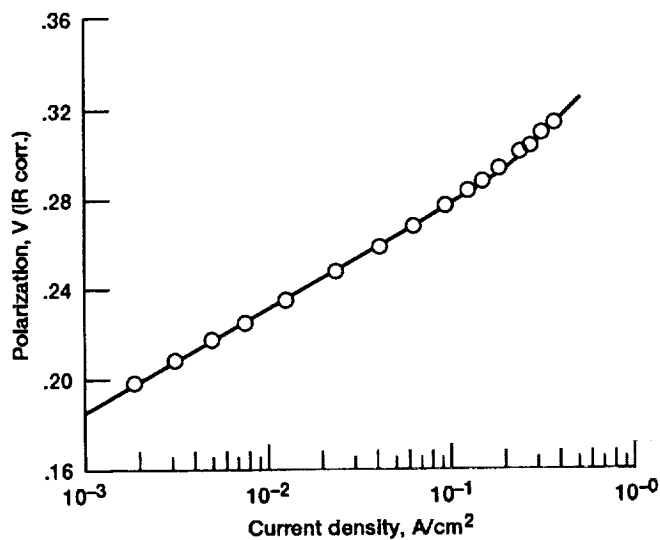


Figure 7.—Tafel plot for $O_2$ reduction at modified electrode B (77.8 °C, 1 atm $O_2$, 30 percent KOH).
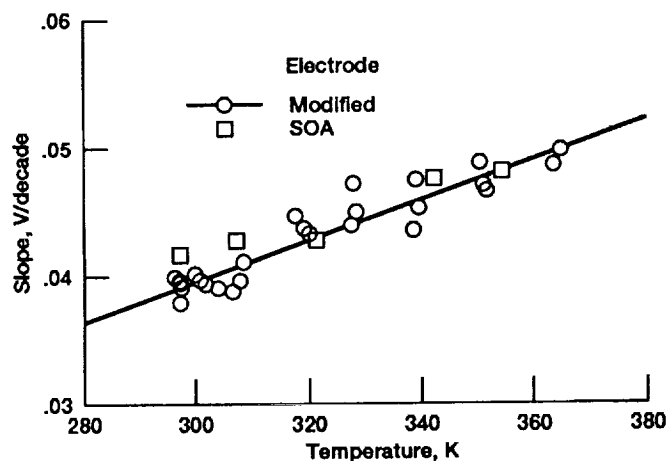


Figure 8.—Tafel slope with respect to temperature for $O_2$ reduction at modified and SOA electrodes in the 0.04 region (1 atm $O_2$, 30 percent KOH).
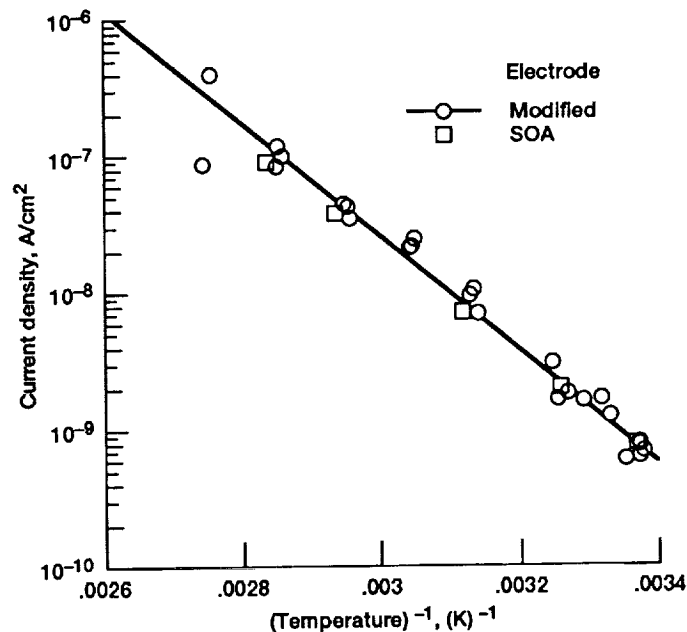


Figure 9.—"Apparent" activation energy plot for $O_2$ reduction at IFC modified electrode in 0.04 V/decade region (1 atm $O_2$, 30 percent KOH).
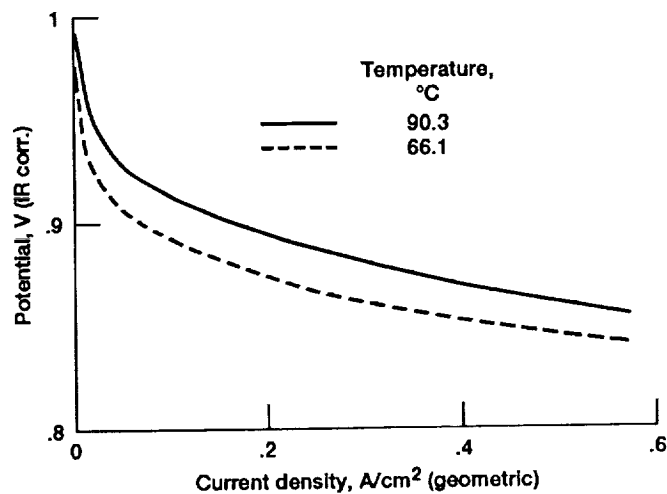


Figure 10.—$O_2$ reduction at electrode A (1 atm $O_2$, 30 percent KOH).

11

# REPORT DOCUMENTATION PAGE

Public reporting burden for this collection of information is estimated to average 1 hour per response, including the time for reviewing instructions, searching existing data sources, gathering and maintaining the data needed, and completing and reviewing the collection of information. Send comments regarding this burden estimate or any other aspect of this collection of information, including suggestions for reducing this burden, to Washington Headquarters Services, Directorate for Information Operations and Reports, 1215 Jefferson Davis Highway, Suite 1204, Arlington, VA 22202-4302, and to the Office of Management and Budget, Paperwork Reduction Project (0704-0188), Washington, DC 20503.

| 1. AGENCY USE ONLY (Leave blank) | 2. REPORT DATE | 3. REPORT TYPE AND DATES COVERED |
|---|---|---|
| | July 1992 | Technical Memorandum |

**4. TITLE AND SUBTITLE**

$O_2$ Reduction at the IFC Modified $O_2$ Fuel Cell Electrode

**5. FUNDING NUMBERS**

WU–506–41–21

**6. AUTHOR(S)**

William L. Fielder, Joseph Singer, Richard S. Baldwin, and Richard E. Johnson

**7. PERFORMING ORGANIZATION NAME(S) AND ADDRESS(ES)**

National Aeronautics and Space Administration
Lewis Research Center
Cleveland, Ohio 44135–3191

**8. PERFORMING ORGANIZATION REPORT NUMBER**

E–7073

**9. SPONSORING/MONITORING AGENCY NAMES(S) AND ADDRESS(ES)**

National Aeronautics and Space Administration
Washington, D.C. 20546–0001

**10. SPONSORING/MONITORING AGENCY REPORT NUMBER**

NASA TM–105691

**11. SUPPLEMENTARY NOTES**

William L. Fielder, Joseph Singer, and Richard S. Baldwin, NASA Lewis Research Center, Richard E. Johnson, LeTourneau University, Longview, Texas 75601. Responsible person, William L. Fielder, (216) 433–5258.

**12a. DISTRIBUTION/AVAILABILITY STATEMENT**

Unclassified - Unlimited
Subject Category 20

**12b. DISTRIBUTION CODE**

**13. ABSTRACT** (Maximum 200 words)

The International Fuel Cell Corporation (IFC) state of the art (SOA) $O_2$ electrode (Au-10% Pt electrocatalyst by weight) is currently being used in the alkaline $H_2$–$O_2$ fuel cell in the NASA Space Shuttle. Recently, IFC has developed an improved $O_2$ electrode, designated as the IFC modified $O_2$ electrode, as a possible replacement for the SOA electrode. In the present study, $O_2$ reduction data were obtained for the modified electrode at temperatures between 23.3 and 91.7 °C. BET measurements gave an electrode BET surface area of about 2070 $cm^2/cm^2$ of geometric surface area. The Tafel data could be fitted to two straight line regions. The slope for the lower region, designated as the 0.04 V/decade region, was temperature dependent, and the transfer coefficient was about 1.5. The "apparent" energy of activation for this region was about 19 kcal/mol. An $O_2$ reduction mechanism for this 0.04 region is presented. In the upper region, designated as the 0.08 V/decade region, diffusion may be the controlling process. Tafel data are presented to illustrate the increase in performance with increasing temperature.

**14. SUBJECT TERMS**

Oxygen electrode; Gold catalyst electrode

**15. NUMBER OF PAGES**

15

**16. PRICE CODE**

A03

| 17. SECURITY CLASSIFICATION OF REPORT | 18. SECURITY CLASSIFICATION OF THIS PAGE | 19. SECURITY CLASSIFICATION OF ABSTRACT | 20. LIMITATION OF ABSTRACT |
|---|---|---|---|
| Unclassified | Unclassified | Unclassified | |

NSN 7540-01-280-5500